JOURNAL OF PHYSICAL ORGANIC CHEMISTRY
J. Phys. Org. Chem. 2007; **20:** 600–609
Published online in Wiley InterScience
(www.interscience.wiley.com) DOI: 10.1002/poc.1215

Theoretical study of optical and electronic properties of the bis-dipolar diphenylamino-endcapped oligoarylfluorenes as promising light emitting materials

Yan-Ling Liu,[1,2] Ji-Kang Feng[1,2]* and Ai-Min Ren[1]

[1]State Key Laboratory of Theoretical and Computational Chemistry, Institute of Theoretical Chemistry, Jilin University, Changchun 130023, People's Republic of China
[2]The College of Chemistry, Jilin University, Changchun 130023, People's Republic of China

Received 20 January 2007; revised 8 April 2007; accepted 11 April 2007

ABSTRACT: We present a detailed study of the structural, electronic, and optical properties of the bis-dipolar emissive oligoarylfluorenes, OF(2)Ar-NPhs. The aim of our quantum-chemical calculations is to investigate the role of the transition and the influence of the optical properties of the various central aryl cores in the oligoarylfluorenes. Geometry optimizations were performed for the ground-state and for the first electronically excited-state. The absorption and emission spectra were calculated using time-dependent density functional theory (TD-DFT). The results show that the HOMO, LUMO, energy gap, ionization potentials (IP), electron affinities (EA) and reorganization energy (λ) of the oligoarylfluorenes are significantly affected by the electronic withdrawing property and the conjugated length of the central aryl core. Consistently, the stronger the electron withdrawing strength, the lower the LUMO energy is. This thus improves the electron-accepting and transporting properties by the low LUMO energy levels. The absorption and emission spectra of this series of bis-dipolar molecules exhibit red shifts to some extent by the electronic nature of the electron affinitive central core in the oligoarylfluorenes. All the calculated results show that the oligoarylfluorenes are promising as useful light emitting materials for OLEDs. Copyright © 2007 John Wiley & Sons, Ltd.

KEYWORDS: oligoarylfluorenes; IP; EA; TD-DFT

INTRODUCTION

Phenyl-based π-conjugated oligomers constitute an active component of organic light emitting diodes (OLEDs) since they exhibit unique and interesting optoelectronic properties.[1–3] As a result, over the past few years, a wide range of functionalized π-conjugated oligomers have been designed and synthesized to tune the desirable optical and electronic properties and to enhance the processing and morphological properties.[4–6] Among these oligomers, oligofluorenes, which consist of an important class of π-conjugated oligomers, are extensively explored for optoelectronic and photonic applications in terms of their electroluminescence,[7–9] liquid crystalline,[10,11] and two-photon absorption properties.[12] It is well known that the device performance of OLEDs depends on the efficient and balanced charge injection, good and comparable mobility for both holes and electrons, and a high luminescence quantum yield.[13–16] Although fluorene-based oligomers show great potential as highly stable and efficient blue emissive materials for OLEDs, a large hole-injection barrier often limits its device efficiency.

Recently much effort has been devoted by Wong and others[17–24] in the phenyl-based π-conjugated oligomers, especially the oligomers with end-capping of diphenylamino groups. Wong and Tao report first a series of bis-dipolar emissive oligoarylfluorenes[17] that bear an electron affinitive core, dibutylfluorene as conjugated bridges, and diphenylamino as end-caps constituting D–π–A–π–D type bis-dipolar molecules, which have a low first ionization potential, high thermal stability, and good amorphous morphological stability. Moreover, these bis-dipolar oligoarylfluorenes possess no or a very small net dipole moment and good luminescence properties that their emissive colors can span almost the full UV–Vis spectrum through incorporating different central aryl such as phenylene, oligothiophenes, dibenzothiophene, etc. Therefore, these oligoarylfluorenes are promising for application in OLEDs as efficient emitters.

**Correspondence to:* J.-K. Feng, State Key Laboratory of Theoretical and Computational Chemistry, Institute of Theoretical Chemistry, Jilin University, Changchun 130023, People's Republic of China.
E-mail: JiKangf@yahoo.com

Abbreviations used: D, dibutylfluorene; π, diphenylamino; A, aromatic ring; Δ_{H-L}, HOMO–LUMO gap; E_g, optical band gap; IPi, onization potential; EA, electron affinity.

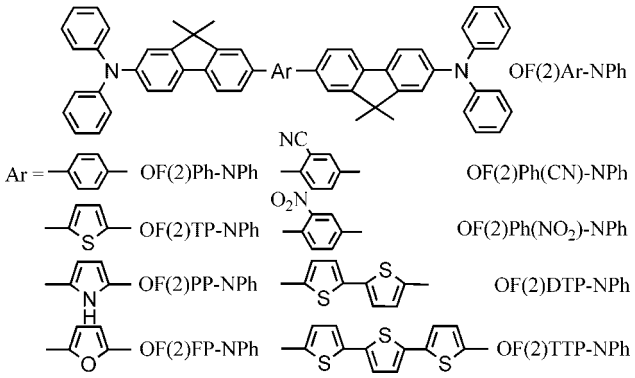

Figure 1. Sketch map of the structures of OF(2)Ar-NPhs. (ChemDraw Ultra 8.0)

In parallel to recent experimental work on the oligomers, theoretical efforts have indeed begun to constitute an important source of valuable information, complementing the experimental studies in the characterization of the nature and the properties of the ground-states and lowest electronically excited states.[25–30] In fact, this type of molecular design or emissive materials applied in OLED applications is largely unexplored, therefore it seems an attractive goal for us to perform a detailed theoretical investigation on these oligoarylfluorenes. Here, we studied in detail a series of bis-dipolar diphenylamino-endcapped oligoarylfluorenes, OF(2)Ar-NPhs (the sketch map of the structures is depicted in Fig. 1) by density functional theory (DFT) methods. The theoretical investigation on the ionization potentials (IP), electron affinities (EA), and band gaps of these oligoarylfluorenes is very instrumental in guiding the experimental synthesis. In particular, the influence of substitution and chain-length effect on various optical and electronic properties is the topic of the present work.

COMPUTATIONAL DETAILS

The ground-state geometries of oligoarylfluorenes, as well as their cationic and anionic geometries, were fully investigated using the DFT, B3LYP/6-31G(d). Geometry optimizations in OF(2)Ph-NPh and OF(2)DTP-NPh were restricted to C_i symmetry. TD-DFT//B3LYP/6-31G(d) calculations of the vertical excitation energies and the maximal absorption wavelengths λ_{abs} were then performed at the optimized geometries of the ground-states. The lowest singlet excited-state structures were carried out with *ab initio* CIS/3-21G(d). Based on the excited geometries, the emission spectra were calculated by TD-DFT//B3LYP/6-31G(d). In addition, the various properties of the oligoaryfluorenes, such as IP, EA, reorganization energy (λ), HOMO–LUMO gap (Δ_{H-L}), and optical band gap (E_g), are obtained from the computed results and compared to the available experimental data. All calculations were done on the SGI origin 2000 server with the Gaussian03 program package.[31]

RESULTS AND DISCUSSION

Ground-state geometry

The optimized structures of OF(2)Ar-NPhs are plotted in Fig. 2 and the important interring bond lengths, dihedral angles and dipole moments of OF(2)Ar-NPhs are collected in Table 1. In contrast to the oligoarylfluorenes in the literature,[17] OF(2)Ar-NPhs studied in this paper substitute butyl with methyl in fluorene rings for reducing the time of calculation.

The calculated results show that the optimized structures of dibutylfluorenes (D) and diphenylaminos (π) in OF(2)Ar-NPhs do not suffer appreciable variation. In fact, because the dihedral angle between the two phenyl rings in the fluorene segment of the diphenylaminos is fixed by ring-bridged atoms, which tend to keep their normal tetrahedral angles in their ring linkage to keep their quasi-planar conformation, the dihedral angles in them are no more than 1°.[32] The bond lengths and dihedral angles between D and π are similar and the main difference occurs between the two adjacent units, π and A in OF(2)Ar-NPhs, especially for the dihedral angles. It can be noted that the A–π dihedral angle twists largely from −36.5 to −42.8°, −49.0° among OF(2)Ph-NPh, OF(2)Ph(CN)-NPh, and OF(2)Ph(NO_2)-NPh, attributing to the electronic withdrawing properties and increasing steric hindrance by the addition of cyano and nitro substituents on the central phenyl core. Increasing thiophene chain length in OF(2)TP-NPh, OF(2)PhDTP-NPh, and OF(2)PhTTP-NPh leads to only small changes in the inter-ring distances and dihedral angles. Comparing OF(2)Ph-NPh, OF(2)TP-NPh, OF(2)PP-NPh, and OF(2)FP-NPh, one can easily find that the bond lengths and the dihedral angles between π and A decrease basically in the sequence of OF(2)Ph-NPh, OF(2)TP-NPh, OF(2)PP-NPh and OF(2)FP-NPh. Importantly, the dihedral angles in OF(2)FP-NPh are nearly 0°. It reveals that OF(2)FP-NPh has the best planar conformation due to the strong push–pull effect between fluorene ring and furan ring, or it could also be explained as due to a weak interaction between the hydrogen atom of the fluorene ring and the oxygen atom in the furan ring. Furthermore, OF(2)Ar-NPhs have a better planar conformation when the central aryl cores are the five-membered rings, resulting from relieving unfavorable steric interactions of the hydrogen atoms between the aromatic rings in OF(2)Ar-NPhs.

As shown in Table 1, the dipole moments of OF(2)Ar-NPhs are small except OF(2)Ph(CN)-NPh and OF(2)Ph(NO_2)-NPh. The dipole moments of OF(2)Ph(CN)-NPh and OF(2)Ph(NO_2)-NPh are 4.17*D* and 4.11*D*, respectively, and this can be ascribed to the influence of the electronic withdrawing groups on the central phenyl core.

DOI: 10.1002/poc

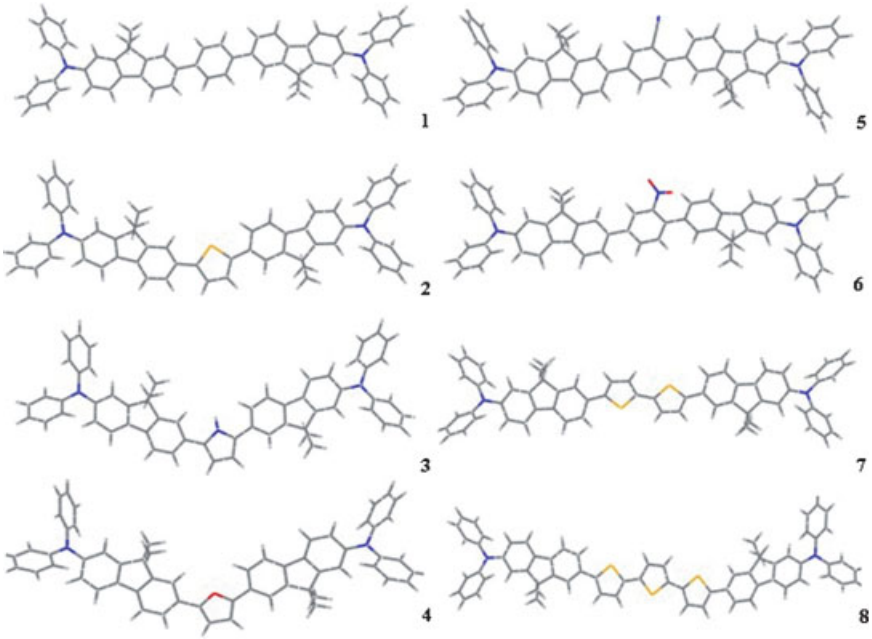

Figure 2. Optimized structures of OF(2)Ar-NPhs(1: OF(2)Ph-NPh, 2: OF(2)TP-NPh, 3: OF(2)PP-NPh, 4: OF(2)FP-NPh, 5: OF(2)Ph(CN)-NPh, 6: OF(2)Ph(NO_2)-NPh, 7: OF(2)DTP-NPh, 8: OF(2)TTP-NPh). (GaussView 3.07)

Frontier molecular orbitals

To gain insight into the excitation properties and the ability of electron or hole transport, we have drawn in Fig. 3 the HOMOs and LUMOs of OF(2)Ar-NPhs. In fact, the first dipole-allowed electron transitions present a strong exclusive HOMO → LUMO character for OF(2)Ar-NPhs (see Subsection 'Absorption spectra'). As expected, the frontier orbitals show π characters and spread over the whole conjugated molecules. In general, the HOMO possesses bonding character and the LUMO holds antibonding character. However, there is antibonding interaction between the two adjacent subunits (D and π, π and A) in the HOMO and bonding interaction in the LUMO, which indicates that the singlet excited states (HOMO → LUMO) for OF(2)Ar-NPhs should be more planar than their ground-states. It is important to note that the electronic cloud distributed in the frontier orbitals of OF(2)Ph(CN)-NPh and OF(2)Ph(NO_2)-NPh have changed much more when employed the electronic withdrawing groups on the central phenyl core. Their HOMO orbitals are mainly localized on the right part of the π-conjugated molecules but LUMO orbitals on the central phenyl core. This suggests that the excitation to the S_1 state corresponding to the promotion of an electron from the HOMO to the LUMO is accompanied with the charge transfer from the right part of the molecules to the central phenyl core.

The calculated HOMO and LUMO levels are presented in Table 2 together with the experimental results. As shown in Table 2, the HOMO energies of OF(2)Ar-NPhs do not alter much on increasing the electronic withdrawing strength or the conjugated length of the central aryl core and the average variation is no more than 0.2 eV.

Table 1. Optimized important interring distances and dihedral angles of OF(2)Ar-nphs with B3LYP/6-31G(d)[a]

	Interring distances (Å)				Dihedral angles (deg.)				
Molecule	D–π	π–A	A–π	π–D	D–π	π–A	A–π	π–D	Dipole moment (*D*)
OF(2)Ph-NPh	1.421	1.483	1.483	1.421	−41.2	36.5	−36.5	41.2	0.00
OF(2)TP-NPh	1.420	1.465	1.465	1.421	−42.0	23.8	−27.2	41.3	0.41
OF(2)PP-NPh	1.421	1.459	1.459	1.421	−41.0	24.3	−21.7	42.4	1.23
OF(2)FP-NPh	1.421	1.453	1.454	1.421	−41.9	−1.5	0.3	41.6	0.54
OF(2)Ph(CN)-NPh	1.419	1.482	1.483	1.420	−39.9	36.7	−42.8	40.9	4.17
OF(2)Ph(NO_2)-NPh	1.419	1.482	1.485	1.420	−39.7	35.5	−49.0	40.8	4.11
OF(2)DTP-NPh	1.420	1.463	1.463	1.420	−40.7	24.2	−24.2	40.7	0.00
OF(2)TTP-NPh	1.420	1.463	1.463	1.420	−41.5	23.6	−25.6	40.7	0.46

[a] D, diphenylamino; π, dimethylfluorene; A, aromatic ring.

DOI: 10.1002/poc

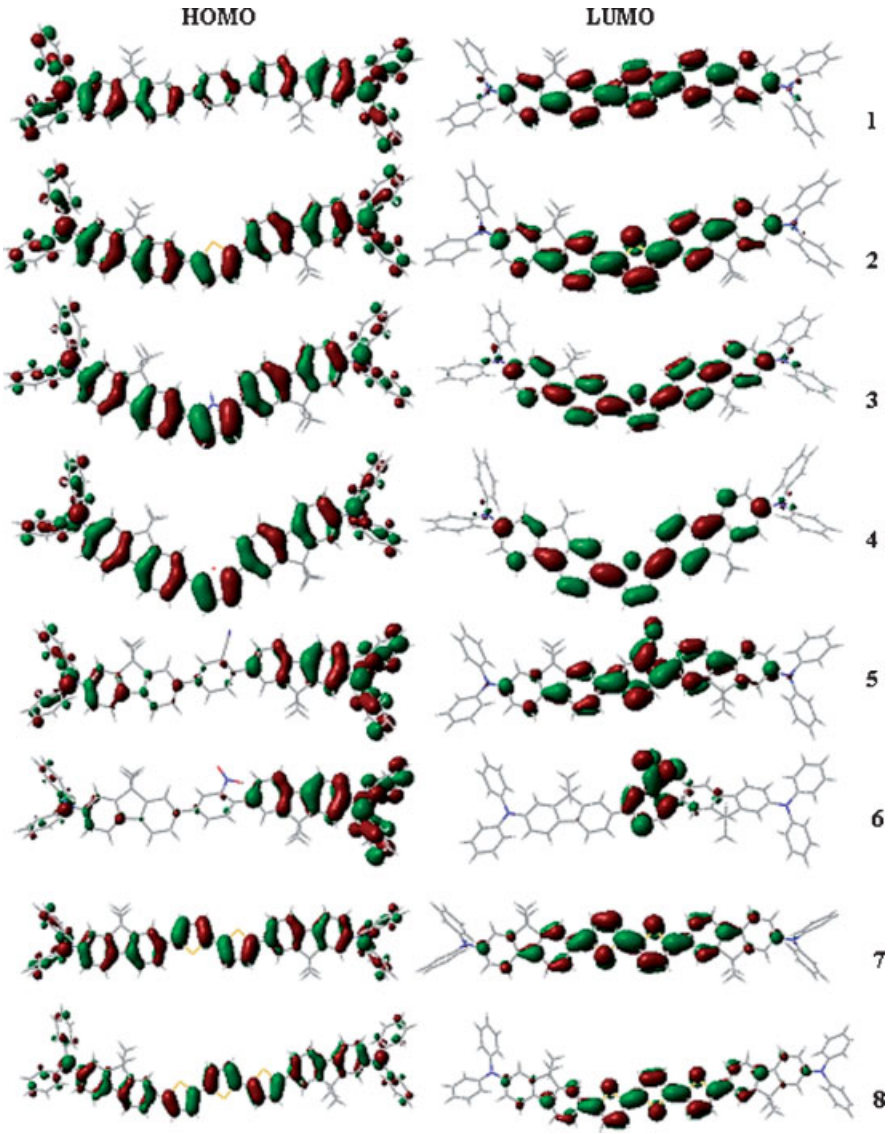

Figure 3. Plots of HOMO and LUMO(calculated at the B3LYP/6-31G(d) level) of OF(2)Ar-NPhs(1: OF(2)Ph-NPh, 2: OF(2)TP-NPh, 3: OF(2)PP-NPh, 4: OF(2)FP-NPh, 5: OF(2)Ph(CN)-NPh, 6: OF(2)Ph(NO_2)-NPh, 7: OF(2)DTP-NPh, 8: OF(2)TTP-NPh). (GaussView 3.07)

Table 2. Comparison between the experimental and calculated HOMO, LUMO energies, HOMO–LUMO Gaps and the lowest excitation energies in eV for OF(2)Ar-nphs[a]

Molecule	$-\varepsilon_{HOMO}$	Exp[b]	$-\varepsilon_{LUMO}$	Exp[c]	Δ_{H-L}	E_g(TD)	Exp[d]
OF(2)Ph-NPh	4.76	5.17	1.28	2.15	3.48	3.08	3.02
OF(2)TP-NPh	4.68	5.14	1.50	2.39	3.18	2.80	2.75
OF(2)PP-NPh	4.53		1.25		3.28	2.88	
OF(2)FP-NPh	4.58		1.44		3.14	2.77	
OF(2)Ph(CN)-NPh	4.86		1.61		3.25	2.90	
OF(2)Ph(NO_2)-NPh	4.85		2.08		2.77	3.07	
OF(2)DTP-NPh	4.66	5.12	1.73	2.51	2.93	2.58	2.61
OF(2)TTP-NPh	4.65	5.11	1.89	2.60	2.76	2.43	2.51

[a] The HOMO and LUMO energies are given in negative and the experimental data (Exp) are taken from Ref. 17.
[b] $E_{1/2}$ *versus* Fc^+/Fc estimated by CV method using a platinum disk electrode as a working electrode, platinum wire as a counter electrode, and SCE as a reference electrode with an agar salt bridge connecting to the oligomer solution. Ferrocene was used as an external standard, $E_{1/2}$ (Fc/Fc+) 0.45 V *versus* SCE.
[c] LUMO = HOMO-energy gap.
[d] Energy gap was estimated from the absorption edge.

DOI: 10.1002/poc

This implies that the different central aryl cores have little effect on weakening the hole-creating properties of OF(2)Ar-NPhs. Such a high HOMO energy level greatly reduces the energy barrier for the hole injection. As a result, OF(2)Ar-NPhs can be used as hole transport/injection materials.

Unlike the HOMO energies, the LUMO energies of OF(2)Ar-NPhs change significantly with the different central aryl cores. The LUMO energies are −1.61 and −2.08 eV in OF(2)Ph(CN)-NPh and OF(2)Ph(NO_2)-NPh, respectively, which are lower than the LUMO energy of OF(2)Ph-NPh(−1.28 eV), indicating that the presence of electronic withdrawing groups on the central phenyl core have significantly enhanced the electron-accepting ability. It is reasonable that the electronic withdrawing groups such as cyano and nitro substituents result in decreasing the LUMO energy. Also the stronger the electron withdrawing strength, the lower the LUMO energy is. Furthermore, we also find that the LUMO energies decrease with increasing thiophene chain length in OF(2)TP-NPh, OF(2)DTP-NPh and OF(2)TTP-NPh. Obviously, OF(2)Ar-NPhs are the good electron-accepting materials.

HOMO–LUMO gaps and the lowest excitation energies

In this section we present the calculated HOMO–LUMO gaps and the lowest excitation energies for OF(2)Ar-NPhs in Table 2. For the sake of comparison, the experimental data are included as well.

Theoretically, the energy gap of the oligoarylfluorene is the orbital energy difference between the HOMO and LUMO, termed the HOMO–LUMO gaps (Δ_{H-L}).[33–35] Experimentally, there are three types of band gaps, namely, the optical band gap, electrochemical band gap and the band gap from a photoelectron spectrum. Among these band gaps, the optical band gap obtained from spectra has the lowest transition (or excitation) energy from the ground-state to the first dipole-allowed excited state, which is an implicit assumption that the lowest singlet excited-state can be described by only one singly excited configuration in which an electron is promoted from the HOMO to the LUMO. In fact, the optical band gap is not the orbital energy difference between the HOMO and LUMO, but the energy difference between the S_0 state and S_1 state. Only when the excitation to the S_1 state corresponds almost exclusively to the promotion of an electron from the HOMO to the LUMO, can the optical band gap be approximately equal to the HOMO–LUMO gap in quantity. To directly compare the experiment, we computed the optical band gaps of OF(2)Ar-NPhs at the TD-DFT level, which are obtained from the absorption spectra and abbreviated E_g. As mentioned above, these optical band gaps of OF(2)Ar-NPhs are the $S_0 \rightarrow S_1$ energy gaps.

For what concerns the transition energies, an overall glance at Table 2 reveals a better agreement of the E_g with the experimental data than the Δ_{H-L} for OF(2)Ar-NPhs. Namely, the discrepancies between the experimental data are 0.06, 0.05, 0.03 and 0.08 eV for E_g and 0.46, 0.43, 0.32 and 0.25 eV for Δ_{H-L} in OF(2)Ph-NPh, OF(2)TP-NPh, OF(2)PhDTP-NPh and OF(2)PhTTP-NPh. This is consistent with the analysis above. Although there are discrepancies between the computed Δ_{H-L} and the experimental data, the variation direction is similar.

As mentioned above, our main purpose of this paper is to investigate the influence of the various electron affinitive central aryl cores onto the oligoarylfluorenes. It can be seen from Table 2 that the band gaps of the oligoarylfluorenes narrowed when modified by the introduction of the electronic withdrawing groups on the central phenyl core and increasing the thiophene chain length. For instance, the band gaps obtained by the HOMO–LUMO gaps and TD-DFT are 3.48 and 3.08 eV for OF(2)Ph-NPh, 3.25 and 2.90 eV for OF(2)Ph(CN)-NPh, 3.18 and 2.80 eV for OF(2)TP-NPh, and 2.76 and 2.43 eV for OF(2)PhTTP-NPh. This hints that the LUMO, HOMO and energy gap of these oligoarylfluorenes are significantly affected by the electronic withdrawing property and the conjugated length of the central aryl core. In other words, we can modify these oligoarylfluorenes by the introduction of the electronic withdrawing groups on the central aryl core and increasing chain length.

Ionization potentials and electron affinities

As mentioned in the Introduction, the good device performance is attributed to the efficient charge injection, the good charge transfer rate and the comparable balance of charge transfer in the OLEDs. We use the ionization potential (IP) and electron affinity (EA) to evaluate the energy barrier for the injection of holes and electrons and employ the reorganization energy (λ) to value the charge transfer (or transport) rate and balance in this paper. The DFT calculated IP, EA, both vertical (v, at the geometry of the neutral molecule) and adiabatic (a, optimized structures for both the neutral and charged molecule), extraction potentials (HEP and EEP for the hole and electron, respectively) that refer to the geometry of the ions, and reorganization energy are listed in Table 3. The relevant calculated detail can be found in Refs 36–38.

To appreciate the influence of the different aromatic rings in the oligoarylfluorenes on the ionization potential and electron affinity, we compare OF(2)Ph-NPh, OF(2)Ph(CN)-NPh and OF(2)Ph(NO_2)-NPh. The energies required to create a hole are about 5.5, 5.6, and 5.6 eV, whereas the extraction of an electron from the anion requires about 0.6, 0.8,and 1.1 eV, respectively. This implies that the presence of the electronic withdrawing groups on the central phenyl core does not affect

DOI: 10.1002/poc

Table 3. IP, EA, extraction potentials and reorganization energies for each molecule (in eV)[a] calculated by DFT

Molecule	IP(v)	IP(a)	Exp	HEP	EA(v)	EA(a)	EEP	λ_{hole}	$\lambda_{electron}$
OF(2)Ph-NPh	5.54	5.48	4.77	5.41	0.35	0.56	0.75	0.13	0.40
OF(2)TP-NPh	5.49	5.38	4.74	5.27	0.53	0.77	0.96	0.22	0.43
OF(2)PP-NPh	5.39	5.27		5.14	0.32	0.49	0.65	0.25	0.33
OF(2)FP-NPh	5.43	5.33		5.22	0.47	0.63	0.79	0.21	0.32
OF(2)Ph(CN)-NPh	5.65	5.60		5.54	0.79	0.84	1.05	0.11	0.26
OF(2)Ph(NO_2)-NPh	5.65	5.60		5.54	0.77	1.07	1.34	0.11	0.27
OF(2)DTP-NPh	5.43	5.33	4.72	5.20	0.78	0.99	1.18	0.13	0.19
OF(2)TTP-NPh	5.38	5.28	4.71	5.18	0.96	1.16	1.32	0.10	0.16

[a] The suffixes (v) indicate vertical and adiabatic values, respectively.

the injection of holes from the anode in light-emitting diodes but largely decrease the LUMO energies, which can better stabilize the anions and more easily accept electrons.

Furthermore, we also compare OF(2)TP-NPh, OF(2)PhDTP-NPh and OF(2)PhTTP-NPh. It can be seen that the EA fall more sharply than the IP with increasing thiophene chain length, which is in accord with the analysis from the energies of the HOMOs and LUMOs. It means that the IP (vertical and adiabatic) slightly fall but the EA (vertical and adiabatic) largely increase the sequence of OF(2)TP-NPh, OF(2)PhDTP-NPh and OF(2)PhTTP-NPh. These results further support these oligoarylfluorenes which can easily be modified or tuned by the use of various central aryl cores. Experimental determination of IP values for organic materials is difficult. It has been suggested by Jenekhe *et al.* [39,40] that a fair estimation of IP can be derived from cyclic voltammetry by taking IP (eV) $= E^{ox}_{onset}$ (vs. SCE) $+ 4.4$.[39,40] Although the IP values for OF(2)Ph-NPh, OF(2)TP-NPh, OF(2)PhDTP-NPh and OF(2)PhTTP-NPh in the experiment are about 4.7 eV, and lie 0.7 eV lower than the calculated data, the variation direction is similar.

As we all know, extensive experimental evidence proves rational that most of the conjugated oligomers and polymers are assumed to transport charge at room temperature via a thermally activated hopping-type mechanism.[41–44] The hole-transfer process between adjacent segments can be summarized as follows:

$$M^+ + M \rightarrow M + M^+$$

where M represents the neutral species undergoing charge transfer and the M^+ species contains the hole. According to the Marcus/Hush theory,[45–48] if the temperature is sufficiently high to treat vibrational modes classically, the hole (or electron) charge transfer rate can be calculated using the following equation, assuming that hole traps are degenerate:

$$k_{hole} = \left(\frac{\pi}{\lambda \kappa_b}\right)^{1/2} \frac{V^2}{\hbar} \exp\left(-\frac{\lambda}{4k_b T}\right) \quad (1)$$

where T is the temperature, k_b is the Boltzmann constant, λ is the reorganization energy due to geometric relaxation accompanying charge transfer, and V is the electronic coupling matrix element between the two species, dictated largely by orbital overlap. Obviously, it can be seen from the Eqn 1 that the efficient charge transfer mostly rests with the value of λ. The reorganization energy λ (here it is the internal reorganization energy due to ignoring any environmental relaxation and changes) for hole transfer can be expressed as follows:[44]

$$\lambda = \lambda_{\gtrless} + \lambda_+ = (\epsilon^*_{\gtrless} - \epsilon_{\gtrless}) + (\epsilon^*_+ - \epsilon_+) \quad (2)$$

As illustrated in Fig. 4, E_0 and E_+ represent the energies of the neutral and cation species in their lowest energy geometries, respectively, while $E_0{}^*$ and $E_+{}^*$ represent the energies of the neutral and cation species with geometries of the cation and neutral species, respectively. The calculated λ_{hole} and $\lambda_{electron}$ are also reported in Table 3. The λ_{hole} slightly change for OF(2)Ar-NPhs, but the $\lambda_{electron}$ decrease in a large degree. For example, the $\lambda_{electron}$ varies from 0.40 eV to 0.26 eV, 0.27 eV in OF(2)Ph-NPh, OF(2)Ph(CN)-NPh and OF(2)Ph(NO_2)-NPh and from 0.43 eV to 0.19 eV, 0.16 eV in OF(2)TP-NPh, OF(2)PhDTP-NPh and OF(2)PhTTP-NPh. This indicates that the combination with the electronic withdrawing groups on the central phenyl core or increasing thiophene chain length will improve both the electron transfer rate and the charge transfer balance, thus further enhancing the device performance of OLEDs.

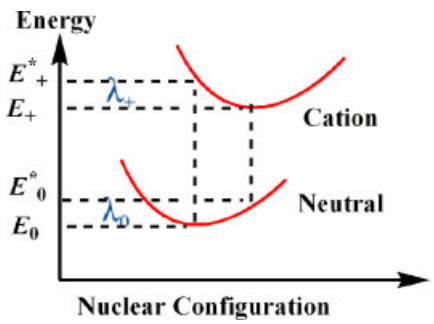

Figure 4. Internal reorganization energy for hole transfer. (ChemDraw Ultra 8.0) This figure is available in color online at www.interscience.wiley.com/journal/poc

DOI: 10.1002/poc

Table 4. Electronic transition data obtained by TD-DFT for OF(2)Ar-nphs at the B3LYP/6-31G(d) optimized geometry

Molecule	Electronic transitions	λ^{abs}_{max} (nm)	Exp[a]	f	Exp[a]	Main configurations	
OF(2)Ph-NPh	$S_0 \rightarrow S_1$	402.75	381	1.95	8.25	HOMO $\rightarrow$ LUMO	0.67
	$S_0 \rightarrow S_2$	378.44		0.00		$HOMO_{-1} \rightarrow$ LUMO	0.67
	$S_0 \rightarrow S_3$	340.83		0.00		HOMO $\rightarrow LUMO_{+1}$	0.66
OF(2)TP-NPh	$S_0 \rightarrow S_1$	442.96	390	2.04	7.29	HOMO $\rightarrow$ LUMO	0.67
	$S_0 \rightarrow S_2$	400.10		0.03		$HOMO_{-1} \rightarrow$ LUMO	0.69
	$S_0 \rightarrow S_3$	352.71		0.05		HOMO $\rightarrow LUMO_{+1}$	0.67
OF(2)PP-NPh	$S_0 \rightarrow S_1$	430.32		2.15		HOMO $\rightarrow$ LUMO	0.67
	$S_0 \rightarrow S_2$	374.72		0.09		$HOMO_{-1} \rightarrow$ LUMO	0.68
	$S_0 \rightarrow S_3$	360.14		0.13		HOMO $\rightarrow LUMO_{+1}$	0.67
OF(2)FP-NPh	$S_0 \rightarrow S_1$	447.92		1.98		HOMO $\rightarrow$ LUMO	0.67
	$S_0 \rightarrow S_2$	394.54		0.10		$HOMO_{-1} \rightarrow$ LUMO	0.68
	$S_0 \rightarrow S_3$	358.32		0.19		HOMO $\rightarrow LUMO_{+1}$	0.67
OF(2)Ph(CN)-NPh	$S_0 \rightarrow S_1$	428.87		1.35		HOMO $\rightarrow$ LUMO	0.68
	$S_0 \rightarrow S_2$	407.05		0.04		$HOMO_{-1} \rightarrow$ LUMO	0.69
	$S_0 \rightarrow S_3$	361.53		0.30		HOMO $\rightarrow LUMO_{+1}$	0.59
OF(2)Ph(NO_2)-NPh	$S_0 \rightarrow S_1$	512.93		0.17		HOMO $\rightarrow$ LUMO	0.69
	$S_0 \rightarrow S_2$	481.90		0.02		$HOMO_{-1} \rightarrow$ LUMO	0.70
	$S_0 \rightarrow S_3$	404.52		1.36		HOMO $\rightarrow LUMO_{+1}$	0.62
OF(2)DTP-NPh	$S_0 \rightarrow S_1$	480.48	424	2.45	7.00	HOMO $\rightarrow$ LUMO	0.67
	$S_0 \rightarrow S_2$	429.46		0.00		$HOMO_{-1} \rightarrow$ LUMO	0.69
	$S_0 \rightarrow S_3$	386.41		0.32		$HOMO_{-2} \rightarrow$ LUMO	0.67
OF(2)TTP-NPh	$S_0 \rightarrow S_1$	510.85	441	2.67	6.76	HOMO $\rightarrow$ LUMO	0.66
	$S_0 \rightarrow S_2$	453.43		0.02		$HOMO_{-1} \rightarrow$ LUMO	0.69
	$S_0 \rightarrow S_3$	414.05		0.28		$HOMO_{-2} \rightarrow$ LUMO	0.67

[a] Measured in $CHCl_3$ (Ref. 17).

Absorption spectra

We have optimized the geometry to obtain the absorption spectra of the singlet–singlet electronic transition of OF(2)Ar-NPhs at the TD-DFT//B3LYP/6-31G(d) level. Table 4 lists out the transition energies, oscillator strengths and main configurations for the most relevant first three singlet excited states in OF(2)Ar-NPhs. It can be seen that our calculated absorption wavelengths are higher than the experimental results. This large discrepancy may be related to using a small basis set, substituting butyl with methyl in fluorene rings for reducing the time of calculation and neglecting completely the solvent effects. In addition, although TD-DFT is a good tool for predicting the absorption spectra of molecules, this method has defects when studying extended systems. Frequently, the optical properties reach saturation quickly for short chain lengths, whereas the orbital energies continue to change for longer oligomers. It is known that the exchange–correlation (XC) functionals must decrease with increasing chain length.[49,50] However, the results can still reflect some variation trend because the atomic structures of the molecules are alike and calculated with the same methods and basis sets.

Obviously, all the electronic transitions contributed from the oligoarylfluorene core are the $\pi \rightarrow \pi^*$ type and this excitation to the S_1 state corresponds almost exclusively to the promotion of an electron from the HOMO to the LUMO, except OF(2)Ph(NO_2)-NPh. The oscillator strength (f) of the $S_0 \rightarrow S_1$ electronic transition is large in each oligoarylfluorene. The excitation to S_3 dominates the promotion of an electron from the HOMO to the $LUMO_{+1}$ in OF(2)Ph(NO_2)-NPh, which may result from the influence of the strong electronic withdrawing group on the central phenyl core, nitro substituent.

Moreover, we also find in Table 4 that with the chain length extension the absorption wavelengths increase progressively in OF(2)TP-NPh, OF(2)PhDTP-NPh, and OF(2)PhTTP-NPh, presenting the red shifts. This is reasonable because the HOMO $\rightarrow$ LUMO transition is predominant in the $S_0 \rightarrow S_1$ electronic transition and, as the analysis above shows, with the extension of molecular size, the HOMO $\rightarrow$ LUMO gaps decrease.

Properties of excited structures and the emission spectra

In this paper, the excited-state properties of OF(2)Ar-NPhs were investigated by configuration interaction singles (CIS) method. We optimize only OF(2)Ph-NPh, OF(2)TP-NPh, OF(2)PP-NPh, and OF(2)FP-NPh by CIS/3-21G(d) and compared to their ground structures by HF/3-21G(d), because the calculation of excited-state properties requires significantly more computational effort than is needed for the ground-states and is dramatically constrained by the size of the molecules. Interestingly, the main characteristics of the frontier orbitals by HF/3-21G(d) are the same as those by B3LYP/6-31G(d). For

DOI: 10.1002/poc

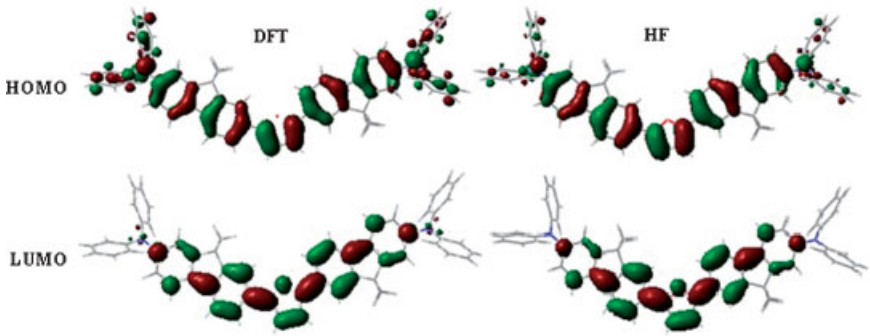

Figure 5. Plots of HOMO and LUMO calculated by HF/3-21G(d) and DFT//B3LYP/6-31G(d) levels of OF(2)FP-NPh. (GaussView 3.07)

example, as shown in Fig. 5, the electronic cloud distributed in the front orbitals is similar. Since the lowest singlet state corresponds to an excitation from the HOMO to the LUMO in OF(2)Ph-NPh, OF(2)TP-NPh, OF(2)PP-NPh and OF(2)FP-NPh, we explore the bond-length variation by analyzing the HOMO and LUMO. As shown in Fig. 3, Table 5 and Table 6, the HOMO possesses an antibonding character between the two adjacent subunits, D and π or A and π, but the LUMO holds an inter-ring bonding character, which is also reflected in the shortening of the corresponding inter-ring CC distances in the excited states. For example, the π–A bond length for OF(2)Ph-NPh in the ground-state is 1.489 Å, but 1.436 Å in the excited state. These geometrical changes due to electron excitation can be supported from Ref. 25 where higher computational levels for the geometry optimizations in the ground and excited states have been used. In Ref. 25, the electronic excitation leads to the large contraction of the inter-ring bonds of methylene-bridged oligofluorenes.

The dihedral angles between two adjacent units rotate to some extent, especially between π and A. The π–A and π–D dihedral angles decrease from 49.8°, 44.4° to 16.3°, 38.0° in OF(2)Ph-NPh, respectively. In fact, there are similar structural variations in OF(2)Ph-NPh, OF(2)TP-NPh, OF(2)PP-NPh, and OF(2)FP-NPh. All the π–A and A–π dihedral angles are about 0° in OF(2)TP-NPh, OF(2)PP-NPh and OF(2)FP-NPh. It is obvious that the excited structure has a better coplanar conformation for these oligoarylfluorenes. Namely, the conjugation of these oligoarylfluorenes is better in the excited structures, which is consistent with the estimation from the character of the frontier orbitals.

In this study, the emission wavelengths are computed by TD-DFT//B3LYP/6-31G(d) and the results are compared to the experimental data. The calculated results show that on going from OF(2)Ph-NPh to OF(2)PP-NPh, OF(2)FP-NPh and OF(2)TP-NPh the λ^{em} exhibits large red shifts, $466.84 < 486.11 < 498.74 < 517.81$ nm and unexpectedly large Stoke's shift (about 64, 43, 68, 70 nm,

Table 5. Optimized important interring distances and dihedral angles of OF(2)Ar-nphs with HF/3-21G(d)[a]

	Interring distances (Å)				Dihedral angles (deg.)				
Molecule	D–π	π–A	A–π	π–D	D–π	π–A	A–π	π–D	Dipole moment (*D*)
OF(2)Ph-NPh	1.422	1.489	1.489	1.422	−44.4	49.8	−49.8	44.4	0.00
OF(2)TP-NPh	1.421	1.474	1.474	1.421	−43.4	41.2	−41.9	44.3	0.51
OF(2)PP-NPh	1.422	1.466	1.466	1.422	−44.0	34.3	−34.3	44.1	1.60
OF(2)FP-NPh	1.421	1.456	1.456	1.421	−43.2	0.1	0.0	43.4	0.69

[a] D, diphenylamino; π, dimethylfluorene; A, aromatic ring.

Table 6. Optimized important interring distances and dihedral angles of OF(2)Ar-nphs with CIS/3-21G(d)[a]

	Interring distances (Å)				Dihedral angles (deg.)				
Molecule	D–π	π–A	A–π	π–D	D–π	π–A	A–π	π–D	Dipole moment (*D*)
OF(2)Ph-NPh	1.413	1.436	1.436	1.413	−38.0	16.3	−16.3	38.0	0.00
OF(2)TP-NPh	1.415	1.411	1.411	1.415	−38.8	0.0	0.0	38.7	0.50
OF(2)PP-NPh	1.417	1.409	1.409	1.417	−41.1	3.9	−3.7	41.1	1.31
OF(2)FP-NPh	1.415	1.398	1.399	1.415	−39.3	0.0	0.0	39.2	0.66

[a] D, diphenylamino; π, dimethylfluorene; A, aromatic ring.

DOI: 10.1002/poc

respectively). This is because of a stronger push–pull effect between the fluorene ring and the central aryl core or the more planar conformation in the excited states. Furthermore, similar to absorption spectra, the emission peaks with the strongest oscillator strength are all assigned to $\pi \rightarrow \pi^*$ character arising from the HOMO to LUMO transition in the four oligoarylfluorenes.

CONCLUSIONS

A systematic theoretical study has been performed on fluorene-based oligoarylfluorenes in this work. All the oligoarylfluorenes show more or less twisted structures because of the electronic nature of the various central aryl cores. The frontier molecular orbitals were spread over the whole π-conjugated molecules. The HOMO possesses an antibonding character and the LUMO holds a bonding character between the two adjacent subunits, which may explain that the excited-state structures of OF(2)Ar-NPhs have a better coplanar conformation than the ground-state structures. Importantly, the introduction of the electronic withdrawing groups on the central phenyl core or increasing thiophene chain length resulted in decreased LUMO energies; consequently, the electron-accepting ability has significantly enhanced. Excitation to the S_1 state corresponds almost exclusively to the promotion of an electron from the HOMO to the LUMO. The absorption spectra of OF(2)Ar-NPhs are mainly determined by the nature of the central aryl cores. Both employing the electronic withdrawing groups on the central phenyl core and increasing the thiophene chain length lead to a red shift of the absorption peak (corresponding to the HOMO–LUMO $\pi \rightarrow \pi^*$ transition). In addition, the emission of OF(2)Ar-NPhs also appear red-shifted to some extent.

Finally, the good agreement between the theoretical results and the experimental data implies that it is possible to design and tune the color emission of efficient and potentially useful light emitting materials.

Acknowledgements

This work was supported by the Major State Basis Research Development Program (2002CB 613406), the National Nature Science Foundation of China, and the Key Laboratory for Superamolecular Structure and Material of Jilin University, People's Republic of China.

REFERENCES

1. Klaerner G, Miller RD. *Macromolecules* 1998; **31**: 2007–2009.
2. Klärner G, Lee J-I, Chan E, Chen J-P, Nelson A, Markiewicz D, Siemens R, Scott JC, Miller D. *Chem. Mater.* 1999; **11**: 1800–1805.
3. Thomas KRJ, Jiann TL, Tao Y-T, Ko Chung-Wen. *Chem. Mater.* 2002; **14**: 1354–1361.
4. Zhu Y, Abhishek P, Jenkehe SA. *Chem. Mater.* 2005; **17**: 5225–5227.
5. Wang Z, Shao H, Ye J, Tang L, Lu Ping. *J. Phys. Chem. B* 2005; **109**: 1962–1963.
6. Liu B, Bazan GC. *J. Am. Chem. Soc.* 2006; **128**: 1188–1196.
7. Wong K-T, Chien Y-Y, Chen R-T, Wang C-F, Lin Y-T, Chiang H-H, Hsieh P-Y, Wu C-C, Chou CH, Su YO, Lee G-H, Peng S-M. *J. Am. Chem. Soc.* 2002; **124**: 11576–11577.
8. Katsis D, Geng YH, Ou JJ, Culligan SW, Trajkovska A, Chen SH, Rothberg LJ. *Chem. Mater.* 2002; **14**: 1332–1339.
9. Geng Y, Culligan SW, Trajkovska A, allace JUW, Chen SH. *Chem. Mater.* 2003; **15**: 542–549.
10. Teetsov J, Fox MA. *J. Chem. Mater.* 1999; **9**: 2117–2122.
11. Jo J, Chi C, Hoger S, Wegner G, Yoon DY. *Chem. Eur. J.* 2004; **10**: 2681–2688.
12. Belfield KD, Morales AR, Hales JM, Hagan DJ, VanStryland EW, Chapela VM, Percino J. *Chem. Mater.* 2004; **16**: 2267–2273.
13. Oyaizu K, Iwasaki T, Tsukahara Y, Tsuchida E. *Macromolecules* 2004; **37**: 1257–1270.
14. Peng Q, Lu ZY, Huang Y, Xie MG, Han SH, Peng JB, Cao Y. *Macromolecules* 2004; **37**: 260–266.
15. Yang RQ, Tian RY, Yang W, Cao Y. *Macromolecules* 2003; **36**: 7453–7460.
16. Yang NC, Lee SM, Yoo YM, Kim JK, Suh DH. *J. Polym. Sci. A* 2004; **42**: 1058–1068.
17. Li ZH, Wong MS, Fukutani H, Tao Ye. *Chem. Mater.* 2005; **17**: 5032–5040.
18. Li ZH, Wong MS, Tao Y, Lu J. *Chem. Eur. J.* 2005; **11**: 3285–3293.
19. Wong MS, Li ZH, Shek MF, Chow KH, Tao Y, D'Iorio M. *J. Mater. Chem.* 2000; **10**: 1805–1810.
20. Wong MS, Li ZH, Tao Y, D'Iorio M. *Chem. Mater.* 2003; **15**: 1198–1203.
21. Li ZH, Wong MS, Tao Y, D'Iorio M. *J. Org. Chem.* 2004; **69**: 921–927.
22. Wong MS, Li ZH. *Pure Appl. Chem.* 2004; **76**: 1409–1419.
23. Donat-Bouillud A, Lévesque I, Tao Y, D'Iorio M. *Chem. Mater.* 2000; **12**: 1931–1936.
24. Li Zhong Hui, Shing Man Wong. *Org. Lett.* 2006; **8**: 1499–1502.
25. Lukes V, Aquino A, Lischka H. *J. Phys. Chem. A* 2005; **109**: 10232–10238.
26. Yang L, Liao Y, Feng J-K, Ren A-M. *J. Phys. Chem. A* 2005; **109**: 7764–7774.
27. Yang L, Feng JK, Ren AM, Sun C-C. *Polymer* 2006; **47**: 3229–3239.
28. Yang L, Feng JK, Liao Y, Ren AM. *Polymer* 2005; **46**: 9955–9964.
29. Yang L, Feng JK, Ren AM. *J. Org. Chem.* 2005; **70**: 5987–5996.
30. Yang Li, Ren A-M, Feng J-K, Wang J-F. *J. Org. Chem.* 2005; **70**: 3009–3020.
31. Frisch MJ, Trucks GW, Schlegel HB, Scuseria GE, Robb MA, Cheeseman JR, Montgomery JA, Jr, Vreven T, Kudin KN, Burant JC, Millam JM, Iyengar SS, Tomasi J, Barone V, Mennucci B, Cossi M, Scalmani G, Rega N, Petersson GA, Nakatsuji H, Hada M, Ehara M, Toyota K, Fukuda R, Hasegawa J, Ishida M, Nakajima T, Honda Y, Kitao O, Nakai H, Klene M, Li X, Knox JE, Hratchian HP, Cross JB, Adamo C, Jaramillo J, Gomperts R, Stratmann RE, Yazyev O, Austin AJ, Cammi R, Pomelli C, Ochterski JW, Ayala PY, Morokuma K, Voth GA, Salvador P, Dannenberg JJ, Zakrzewski VG, Dapprich S, Daniels AD, Strain MC, Farkas O, Malick DK, Rabuck AD, Raghavachari K, Foresman JB, Ortiz JV, Cui Q, Baboul AG, Clifford S, Cioslowski J, Stefanov BB, Liu G, Liashenko A, Piskorz P, Komaromi I, Martin RL, Fox DJ, Keith T, Al-Laham MA, Peng CY, Nanayakkara A, Challacombe M, Gill PMW, Johnson B, Chen W, Wong MW, Gonzalez C, Pople JA. Gaussian 03, Revision B.04; Gaussian, Inc.: Pittsburgh, PA, 2003.
32. Burns DM, Iball S. *Proc. Roy. Soc. London Ser. A* 1955; **227**: 200.
33. Hay PJ. *J. Phys. Chem. A* 2002; **106**: 1634–1641.
34. Curioni A, Andreoni W, Treusch R, Himpsel FJ, Haskal E, Seidler P, Heske C, Kakar S, van Buren T, Terminello LJ. *Appl. Phys. Lett.* 1998; **72**: 1575–1577.
35. Hong SY, Kim DY, Kim CY, Hoffmann R. *Macromolecules* 2001; **34**: 6474–6481.
36. Lin BC, Cheng CP, Lao ZPM. *Phys. Chem. A* 2003; **107**: 5241–5251.

DOI: 10.1002/poc

37. Curioni A, Boero M, Andreoni W. *Chem. Phys. Lett.* 1998; **294**: 263–271.
38. Wang I, Estelle BA, Olivier S, Alain I, Baldeck PL. *J. Opt. A: Pure Appl. Opt.* 2002; **4**: S258–S260.
39. Kulkarni AP, Tonzola CJ, Babel A, Jenekhe SA. *Chem. Mater.* 2004; **16**: 4556–4573.
40. Zhu Y, Babel A, Jenekhe SA. *Macromolecules* 2005; **38**: 7983–7991.
41. Epstein AJ, Lee WP, Prigodin VN. *Synth. Met.* 2001; **117**: 9.
42. Reedijk JA, Martens HCF, van Bohemen SMC, Hilt O, Brom HB, Michels MAJ. *Synth. Met.* 1999; **101**: 475–476.
43. Mott NF, Davis EA. *Electronic Processes in Non-Crystalline Materials* (2d edn). Oxford University Press: Oxford, 1979.
44. Geoffrey RH, Ratner MA, Marks TJ. *J. Am. Chem. Soc.* 2005; **127**: 2339–2350.
45. Marcus RA. *Rev. Mod. Phys.* 1993; **65**: 599–610.
46. Marcus RA, Eyring H. *Annu. Rev. Phys. Chem.* 1964; **15**: 155–196.
47. Hush NS. *J. Chem. Phys.* 1958; **28**: 962.
48. Marcus RA. *J. Chem. Phys.* 1956; **24**: 966.
49. Grimme S, Parac M. *Chem. Phys. Chem.* 2003; **4**: 292–295.
50. Ortiz RP, Delgado MCR, Casado J, Herna'ndez V, Kim OK, Woo HY, Navarrete LL. *J. Am. Chem. Soc.* 2004; **126**: 13363–13376.

DOI: 10.1002/poc